Fatma Uyar[a], Seth R. Wilson[a], Jason Gruber[b], Sukbin Lee[a], Stephen Sintay[a,c], Anthony D. Rollett[a], David J. Srolovitz[d]

[a] Carnegie Mellon University, Materials Science and Engineering Department, Pittsburgh, USA
[b] Bettis Atomic Laboratory, West Mifflin, USA
[c] now a graduate research assistant at the Los Alamos National Laboratory, Los Alamos, USA
[d] Yeshiva University, New York, USA

Testing a curvature driven moving finite element grain growth model with the generalized three dimensional von Neumann relation

Dedicated to Professor Dr. Günter Gottstein on the occasion of his 65th birthday

The von Neumann–Mullins relation has been extended to higher dimensions by MacPherson and Srolovitz. Their exact solution relates the rate of volume change of an individual grain in a 3-dimensional isotropic polycrystal to its mean width and total length of triple lines (assuming isotropic boundaries). The objective of this study is to verify that grains in a moving finite element grain growth model obey this law. Algorithms have been developed in order to calculate mean width of individual grains in digital microstructures for which the grain structure is discretized with both volumetric and surface meshes. Theoretical rate predictions were obtained from the measured mean widths and triple line lengths. Good agreement was found between growth rates measured in the simulations and the predictions of MacPherson–Srolovitz theory for the cases of an isolated shrinking sphere, individual grains in a digitally generated coarse polycrystal, and individual grains in a microstructure reconstructed from serial sectioning of stabilized cubic zirconia. Departures from this relationship appeared to be related to the grain shape.

Keywords: Grain growth; Finite element; Mean width; Simulation

1. Introduction

1.1. Isotropic grain growth

The enduring quest in materials science and engineering is to improve our understanding of the relationships between microstructure, processing and properties of materials [1]. In the case of metals and ceramics, the network of grain boundaries defines the (typically) polycrystalline microstructure. It is critically important to have a quantitative understanding of how these polycrystalline microstructures evolve. In two dimensions, the von Neumann–Mullins relation predicts the rate of area change for a grain [2, 3] based on only its topology as quantified by the number of sides:

$$\frac{\mathrm{d}A}{\mathrm{d}t} = -M\gamma\left(2\pi - \sum_{i=1}^{n}\alpha_i\right) = -2\pi M\gamma\left(1 - \frac{1}{6}n\right) \qquad (1)$$

In Eq. (1) above, $\mathrm{d}A/\mathrm{d}t$ is rate of area change, M is grain boundary mobility, γ is the grain boundary energy and α_i is the turning angle at a triple junction. In an isotropic material, grain boundaries meet along triple points at 120° angles and the turning angle is equal to $\pi/3$. Thus, in this 2-D curvature driven model, shrinkage or growth is predicted based on the number of nearest neighbors of a grain. There have been efforts to find a similar relationship for the grain growth dynamics in three-dimensional polycrystals. Glazier analyzed individual grains in a 3D Monte Carlo model and, in making a linear fit between growth rate and facet number, emphasized the importance of topology [4]. Mullins' three-dimensional bubble evolution analysis [5] made a simplifying assumption that all faces have five edges and obtained a mildly non-linear relationship between growth rate and the number of faces (nearest neighbors). Although more complicated in detail, Mullins' growth function is approximately proportional to the square root of the number of facets. Hilgenfeldt et al. developed an analytical relationship for the growth function [6] based on an assumption of spherical caps on each facet; as in Mullins' result, the growth function tends towards a square root behavior at large facet number. Glicksman developed a relationship for average n-hedra in his capillarity driven growth study [7]; based on this result for idealized shapes, Rios and Glicksman go on to derive grain size distributions by assuming that growth rates are proportional to the square root of the facet number [8]. MacPherson–Srolovitz have generalized the von Neumann–Mullins relationships to three and higher dimensions [9]. According to the MacPherson–Srolovitz relation for an isotropic polycrystal (in the sense of uniform grain boundary energy), in three dimensions, the rate of volume change of a grain can be calculated by

determining the mean width and total length of triple lines. The difference between the *mean width, L,* of the grain, and one-sixth of the sum of the length of triple lines, *e*, predicts whether the grain will shrink or grow.

$$\frac{\mathrm{d}V}{\mathrm{d}t} = -2\pi M\gamma\left(L - \frac{1}{6}\sum_i e_i\right) \tag{1}$$

Wang and Liu [10] also analyzed individual grain growth rates in a Monte Carlo model and concluded that the data could not be used to distinguish between a linear versus a square root (of facet number) growth law. Recently Barrales–Mora et al. [11] analyzed the growth rate of grains in a vertex model. They concluded that the individual growth rates were in good agreement with the MacPherson–Srolovitz theory but that the previous theories (Hilgenfeldt, Mullins) also fit their results well. Note, however, that they chose to emphasize the topological class by averaging growth rates (within each class) and did not examine in detail the behaviour of individual grains in their polycrystal simulations. Long before these contributions, Cahn [12] derived a similar relationship for convex bodies for which the mean width is equal to the caliper diameter (bar a numerical factor), so it is clear that the major contribution of MacPherson–Srolovitz is to generalize the computation of mean curvature to non-convex objects.

1.2. Mean width of digital microstructures

The reason that the mean width is so useful in grain growth theory is that it measures the integrated mean curvature of an object. Stoyan et al. [13] provides a brief description of mean width based on measure theory. The calculation of mean width, *L*, can be performed using the Crofton formula, where *X* is the object to be measured, *P* is a test plane that is passed through the object in all directions, *n*, and χ is the Euler characteristic (or connectivity number) of the intersection of the body with the test plane:

$$L = 2\int_{s^2} \mathrm{d}\vec{n} \int_R \mathrm{d}s\, \chi\left(X \cap P_{\vec{n},s}\right) \tag{3}$$

For a sphere with diameter *d*, test planes with normals parallel to the line direction *l*, will either not touch the object, therefore resulting in a Euler characteristics of either 0, or touch the object and result in an Euler characteristic of 1. Thus evaluation of the integral will yield the diameter, *d*, and therefore the mean width of a sphere is equal to twice its caliper diameter based on this definition [14]. It is also equal to the integral mean curvature of the object, divided by 2π. For a polyhedron with flat faces and *v* edges, the mean width can be calculated using Eq. (4), where ε is edge length and β is the turning angle, which is positive or negative depending on whether the object is convex or concave along the corresponding edge respectively [9]. The notation for angles and edge lengths is chosen in this fashion to differentiate edges and turning angles along the flat surfaces rather than of the case of triple lines of a grain. The mean width of objects in digital microstructures in a surface mesh can be calculated in this fashion.

$$L = \frac{1}{2\pi}\sum_i^v \varepsilon_i\beta_i \tag{4}$$

Hadwiger has shown [15] that for three-dimensional domains there is one and only one measure in each of one, two and three dimensions that satisfies the additivity law. These unique measures (in 3D) are volume, area and mean width. Therefore, the additivity rule can be employed to calculate mean width in volumetric meshes. In our volumetric meshes, grains are constructed with tetrahedral elements and, from the additivity rule, the mean width, *L*, of a grain can be calculated by adding up the individual mean widths of its tetrahedral elements, subtracting the mean width sum of the triangles at the intersections of tetrahedra and adding up the mean widths of edges of the triangles that lie within the grain.

$$L(\text{Grain}) = \sum L(\text{Tetrahedron}) - \sum L(\text{Triangle}) + \sum L(\text{Edge}) \tag{5}$$

Thus we developed two different methods for calculating the mean width of digital microstructures. For surface meshes, Eq. (4) for polyhedra with flat facets was used and for volumetric meshes, the additivity rule based on Eq. (3) was used.

2. Experimental procedure

2.1. Digital mesh generation

In order to verify the grain growth kinetics of the model, a test case of a spherical grain was used. This spherical grain loses volume and interfacial area while maintaining its shape, assuming curvature-driven boundary motion. Thus the rate of change of interfacial area can be calculated analytically. Following the MacPherson–Srolovitz relation, the rate of change of volume only depends on the mean width since the structure lacks triple lines. In the first discretization of the microstructure, tetrahedral elements are used to approximate the spherical grain; in the second type of discretization, a triangular surface mesh is used to describe the same spherical grain volume, Fig. 1.

The digital polycrystal was generated in order to study the growth rates of the grain network. Regular partitioning of a unit cube into a grid of 50^3 cells was the first step in creating the microstructure. At every cell corner, a node

Fig. 1. Spherical grain embedded inside unit cube. The rate of interfacial area change can be analytically solved using the curvature driven growth relation. Following MacPherson–Srolovitz relation, the rate of volume change is dependant on the mean width since the structure lacks triple lines.

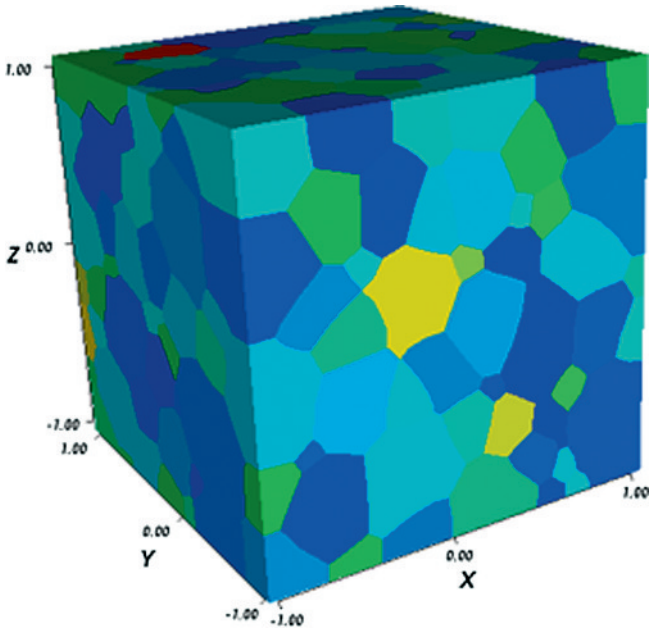

Fig. 2. Digitally generated coarse polycrystal structure. Digitally generated polycrystal structure with 379 grains. The tetrahedral volumetric mesh has 36 007 nodes and 80 581 elements.

was placed and later linked in order to create a regular tetrahedral mesh consisting of 750 000 equal volume elements. 5000 tetrahedra were then randomly chosen as seeds and assigned with individual grain identifiers under the constraint that two different grain centers would not fall onto neighboring tetrahedra. The mesh then was subjected to isotropic grain growth [16] until 379 grains remained, Fig. 2. Several re-meshing steps and mesh quality operations were done periodically in the coarsening process [17] using the Los Alamos Grid Toolbox [18] software package.

The second polycrystal microstructure was based on the voxelized information from a stabilized cubic zirconia sample obtained by serial sectioning with a dual beam FIB-SEM [19]. From the voxelized microstructure, Fig. 3a, a surface mesh was generated using a multi-spin marching cubes algorithm [20]. The resulting surface mesh had 1391 grains with an average of more than 1000 elements per grain, Fig. 3b.

2.2. Simulation of grain growth

The curvature driven grain growth model is based on the interface motion defined by Eq. (6), where v_n denotes the magnitude of the interface normal velocity, M the interface mobility, and $\nabla_n E$ is the total system energy change resulting from an infinitesimal normal displacement of the interface at a given point.

$$v_n = M\nabla_n E \tag{6}$$

The moving finite element method attempts to move mesh nodes so that the equation of motion is satisfied as well as possible at all points on each interface. This naturally leads to minimization of a functional that quantifies the differences between actual and desired nodal velocities, Eq. (7).

$$J = \int_s (v_n - M\nabla_n E)^2 \, \mathrm{d}S \tag{7}$$

over all possible nodal velocities. Here S implies all mobile interfaces discretized by triangles. Additional forces on the nodes are required so that element quality is maintained during mesh motion, and these forces can also be expressed as a functional. Minimization of these functionals with respect to the motion of all nodes lies at the heart of the moving finite element method and the detailed derivation can be found in [21] and Gruber's thesis [17]. This method does not address the need for topological changes during coarsening. The simulation does not use periodic boundary conditions and nodes on the borders of the simulation volume are constrained not to move.

3. Results

3.1. Spherical grain

Spherical grain shrinkage can be solved analytically under the assumption that the normal velocity of each grain interface is equal to the product of curvature, interfacial energy, and mobility (for isotropic boundaries). From this, the rate of change of interfacial area, dA/dt, can be calculated. The surface area of a spherical grain, A, changes at fixed rate,

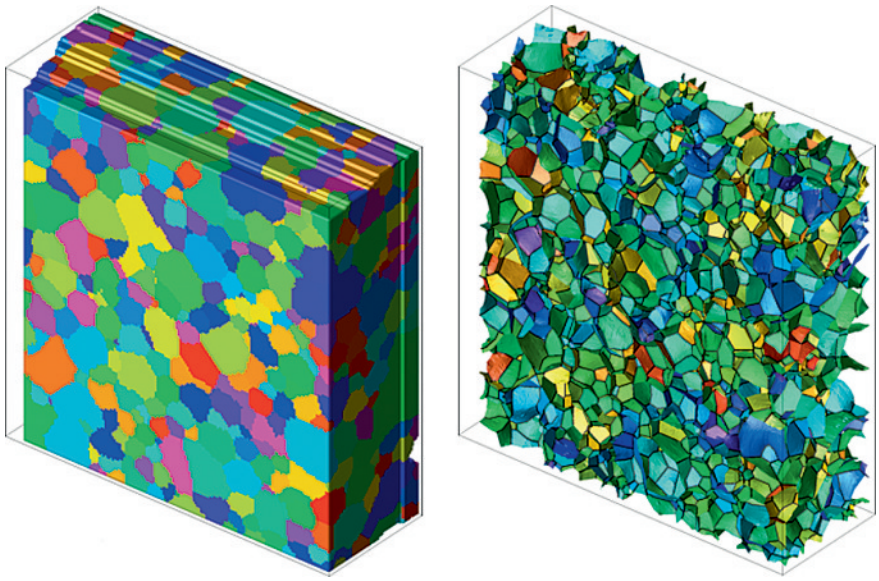

Fig. 3. (a) Voxelized microstructure based on the serial sectioning of zirconia by dual beam FIB/SEM. (b) Surface mesh generated upon the voxelized microstructure. The resulting microstructure has 670 424 nodes and 1 426 683 triangles are covering 1391 grains.

given that the velocity of the interface obeys curvature driven motion, where M is the grain boundary mobility and γ is the grain boundary energy per unit area, Eq. (8).

$$\frac{dA}{dt} = \frac{dA}{dr}\frac{dr}{dt} = 8\pi r\left(-\frac{2M\gamma}{r}\right) = -16\pi M\gamma \tag{8}$$

Furthermore the MacPherson–Srolovitz relation, Eq. (2), shows that the rate of volume change depends only on the mean width since the structure lacks any triple lines.

$$\frac{dV}{dt} = -2\pi M\gamma\left(H(\mathbf{D}) - \frac{1}{6}\sum_i e_i(\mathbf{D})\right)$$
$$= -2\pi M\gamma(H(D)) = -8\pi M\gamma r \tag{9}$$

The volumetric mesh representing the spherical grain is shown in Fig. 1 and the plots in Fig. 4 show the grain volume and interfacial area measured over several time steps. The total time was chosen to be small enough that the volume change in this test and in the polycrystal simulations was less than 0.02 %. Also, M and γ are set to 1 for both cases, which means that the simulations are performed with normalized quantities (as opposed to physical values to represent a particular material). For our rate comparison purposes, no topological changes were needed within this simulation time, which facilitates rate comparison analysis.

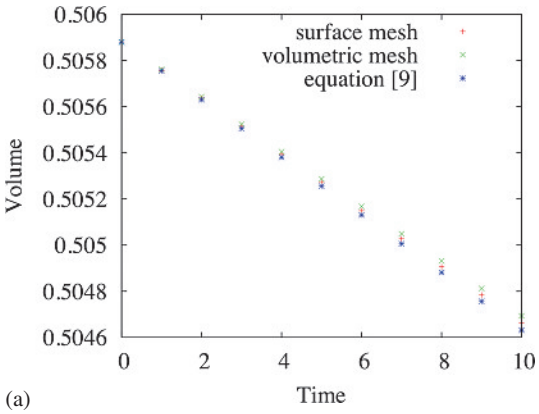

(a)

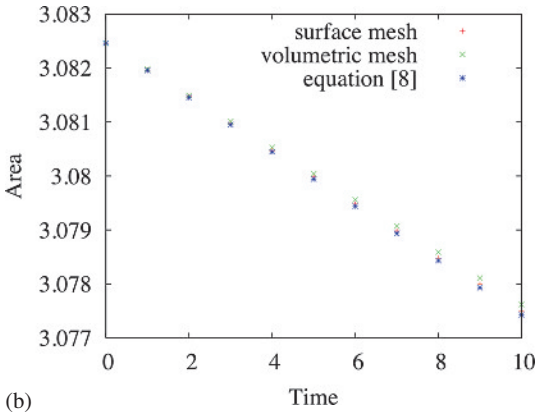

(b)

Fig. 4. Shrinking sphere case: (a) Volume change during the simulation for the volumetric and surface meshes plotted against the predictions from Eq. (9). (b) Interfacial area change during the simulation for the volumetric and surface meshes plotted against the predictions from Eq. (8). Both meshes represent an isolated (island) spherical grain. The slopes of the plots were compared to theoretical rate predictions. The result for the surface mesh is closer to the theoretical prediction because using a surface mesh eliminates the necessity of quality forces for (tetrahedral) elements inside the grains.

Also the short time minimizes the error in applying linear regression to obtain dV/dt as the slope of volume versus time.

Comparison of the slopes of the plots from Fig. 4 showed that the simulation rates are ~5 % and 4 % slower in Fig. 4a and Fig. 4b, respectively, than the theoretical predictions. In the case of the surface mesh, dV/dt and dA/dt measured in simulation differs from the theoretical predictions by 3 %, because using a surface mesh eliminates the necessity of quality forces for tetrahedral elements within the grains.

3.2. Coarse polycrystal

The mean width, L, for each grain in the coarse polycrystal, Fig. 2, is plotted against the cube root of the initial grain volume in Fig. 5a. The linear relationship shows that the mean width is proportional to the sphere equivalent radius or diameter as expected. The best-fit slope is 2.72, which may be compared with the value of approximately 2.4814 for the sphere. Also, by measuring the edge length of the triple lines, the rate of volume change can be predicted using the Srolovitz–MacPherson relation, Eq. (2). dV/dt values measured for each grain over several time steps in the simulations are plotted versus the predicted values in Fig. 5c. The small departure from the 1 : 1 line indicates good agreement between theory and simulation. The outliers from the linear trend are the grains whose mean widths are also among the outliers, as shown in Fig. 5d. Since the relationship between mean width and volume is a measure of shape (just as for the more familiar area:volume ratio) this suggests that departures from standard shapes are correlated with deviations from the MacPherson–Srolovitz relationship, at least in this model. This apparent importance of grain shape motivated Fig. 5b, where we present a new way of characterizing shape by using the basic quantities of volume, area and mean width, i.e. the three quantities that possess the property of additivity. The graph is of the cube root of the volume against the square root of area, both normalized by mean width in order to arrive at dimensionless quantities; this is closely related to the Blaschke diagram [22].

3.3. Measured microstructure of stabilized cubic zirconia

A plot of mean width versus cube root of volume for the sample of stabilized cubic zirconia based on surface mesh is shown before and after two methods of smoothing in Fig. 6a. Linear regression yields fits with r-values of 0.984(initial), 0.989 (MFE) and 0.979 (CLS) respectively. The first smoothing method uses the moving finite elements approach (MFE smoothed), whereas the second method uses a constrained line straightening (CLS) approach. In the constrained line straightening method, each grain boundary line is considered as a string of edges where the two end nodes (typically, triple/quadruple points in space) are fixed. Then a line is drawn from the starting node to the midpoint of next edge. If the distance from the previous node is less than a threshold value, then such a line is drawn to the next edge, otherwise the grain boundary is traced back to the previous line. Then the previous nodes are moved to the equi-distanced points on the line and used to connect the end point to the start point. This process is repeated for all lines across the boundaries and the entire sequence is repeated for as many iterations as are found to

be needed to optimize the structure. A complete description of the method will be detailed in a subsequent publication.

The variation in the proportionality between L and $V^{1/3}$ for the stabilized cubic zirconia case shows that there is a measurable variation in shape during smoothing. The slope in the initial surface is 3.6, whereas the MFE smoothed mesh has 3.09 and the CLS method results in a slope of 3.06. As mentioned above, these values can be compared with the value of 2.481 for spheres and the value of 2.72 found for the simulated polycrystal. Figure 6b shows a plot of growth rates (dV/dt) of individual grains measured from moving finite element simulations of grain growth with different isotropic grain boundary mobilities, against the rate predicted by the MacPherson–Srolovitz theory. To a good approximation, the measured (reduced) mobility is proportional to the mobility used in the model.

Figure 6c, d and e shows histograms of the mean width, volume and area, respectively; note the contrast between the obviously skewed distributions of area and volume, compared to the approximately normal distribution of mean width. Finally Fig. 6f shows a plot of dimensionless shape factors calculated as the cube root of volume versus the square root of area, both normalized by the mean width. Note how both these ratios vary together over similar ranges for both this experimental microstructure and the theoretical one, Fig. 5b.

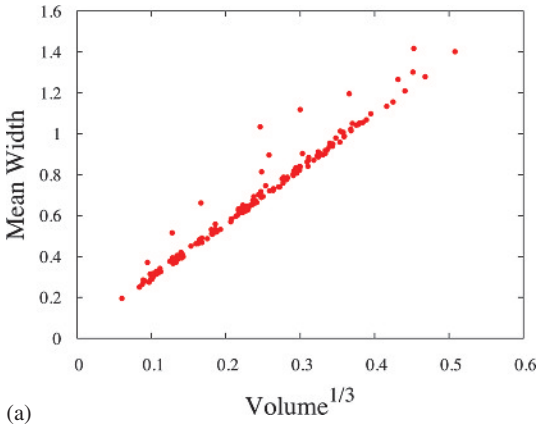

(a)

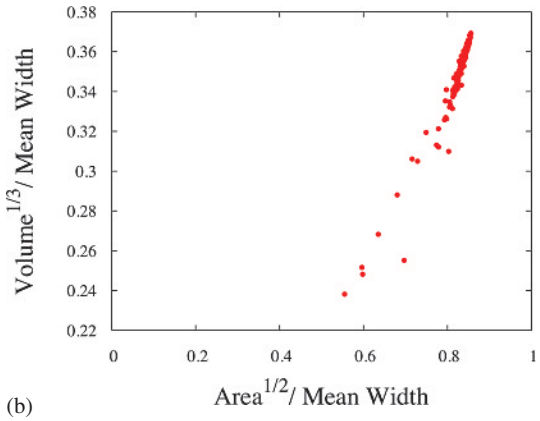

(b)

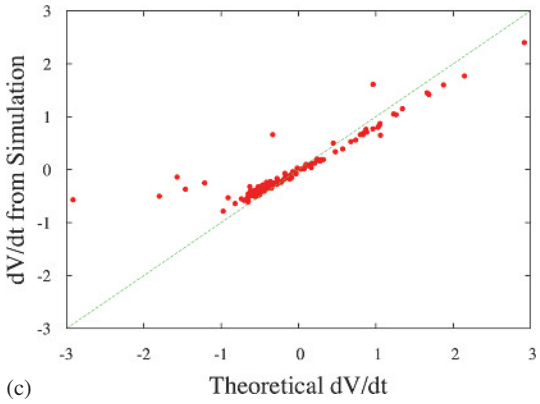

(c)

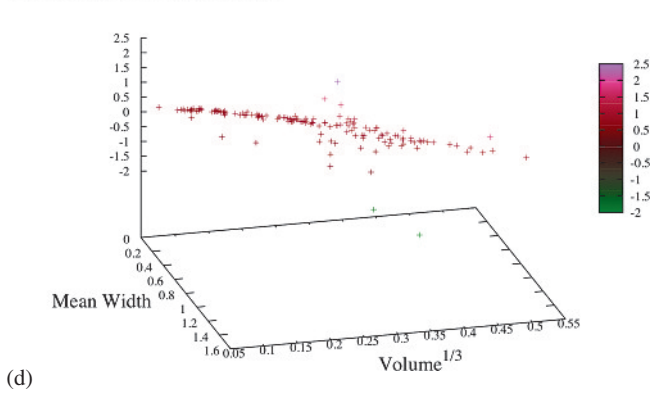

(d)

4. Discussion

The isolated shrinking spherical grain discretized with a volumetric mesh showed that rates for interfacial area and volume change measured in simulation follow the theoretical predictions based on curvature driven grain growth. The rate of shrinkage, however, is slower by $\sim 5\,\%$ than the predictions both in area and volume change. The additional forces for maintaining the mesh quality (i.e. aspect ratios of triangle and tetrahedron elements) retard the interface motion. However, when the same grain is represented by a surface mesh, the difference between the simulation and theoretical rates decreases to 3 % because the absence of internal elements eliminates the necessity for additional forces to maintain tetrahedral volume elements. Note, however, that quality forces are still required in the triangular surface mesh in order to maintain element quality.

The coarse polycrystal results show that mean width data for the interior grains follows the trend for sphere equivalent mean width. There are several grains in the outliers of this trend, which might be due to their distorted shapes before a topological event. The grains overall follow the theoretical rate predictions, except for the outliers from the trendline of mean width versus volume.

The calculations for the measured stabilized cubic zirconia microstructure showed that the constant of proportional-

◀ Fig. 5. Digital polycrystal case: (a) Mean width plotted versus the cube root of the volume; grains that are in contact with the exterior surface of the digitally generated polycrystal are excluded. (b) Plot of cube root of volume divided by mean width against square root of area divided by mean width. (c) Plot of growth rates (dV/dt) of individual grains measured from a moving finite element simulation of grain growth, against the rate predicted by the MacPherson–Srolovitz theory. (d) 3D plot of the ratio of growth rates, versus mean width and the cube root of the volume. The mean width data is proportional to the cube root of volume. The small departure from the 1 : 1 line indicates good agreement between theory and simulation. The outliners in the trend are the grains whose mean widths are also among the outliers. Some grains deviate both + and – from both the shape factor and, at the same time, dV/dt ratio.

ity between L and $V^{1/3}$ varies during smoothing. This suggests that mean width, along with the more familiar volume and surface area, can be used to quantify the degree of smoothing. Experimental techniques offer inherently voxelized structures, which require smoothing before use as a source of data in materials science studies such as grain boundary area as a function of boundary type and so quantitative measures of the quality of the result are important. It is important to state that the authors are not aware of any quantitative measures for quality of surface smoothing beyond standard measures of element quality such as the aspect ratio utilized in this work.

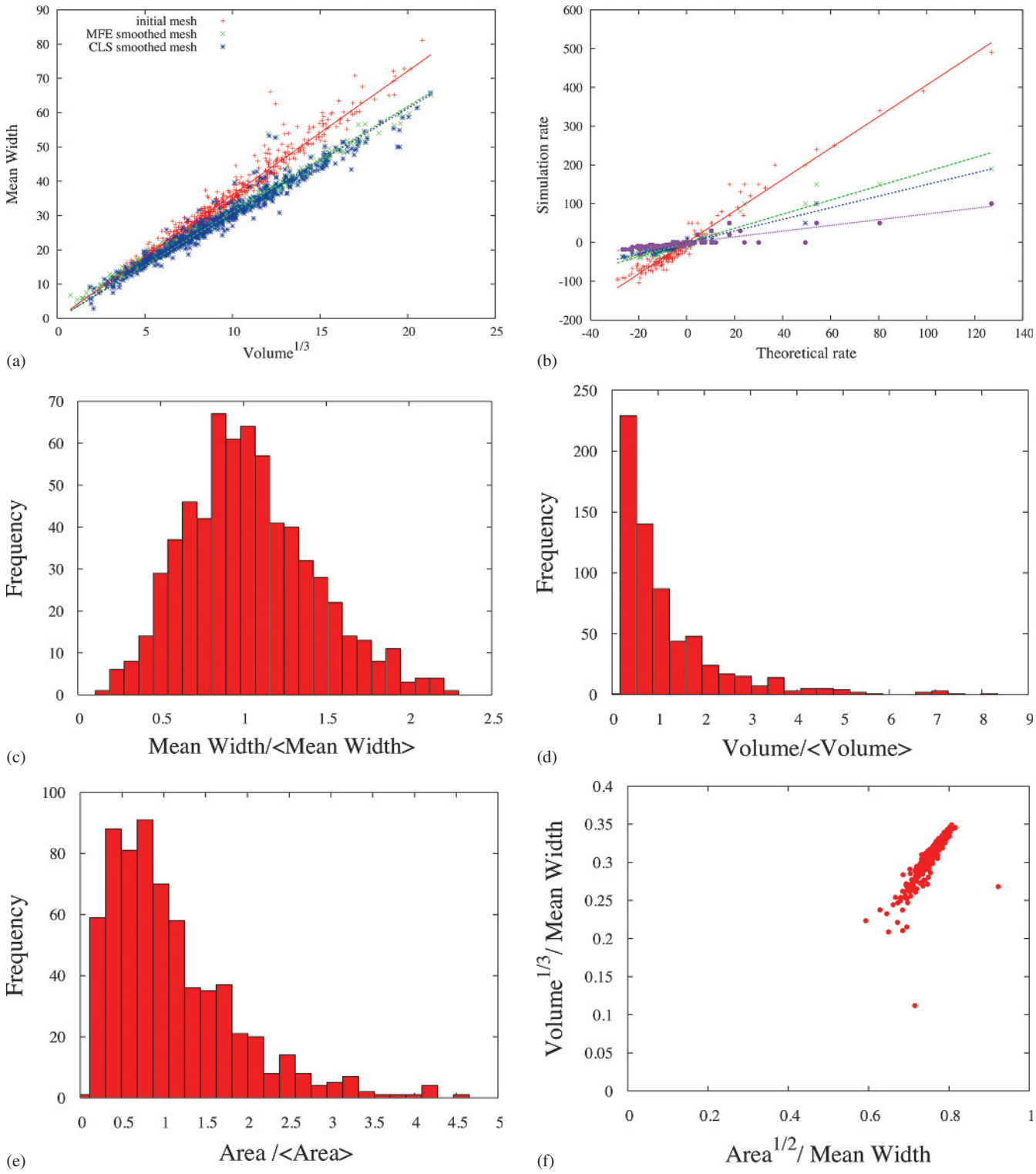

Fig. 6. (a) Mean width plotted versus cube root of the volume, for the surface mesh based on the serial section dataset for zirconia before and after two different methods of smoothing. For comparison, the slope for the sphere is 2.481. (b) Plot of growth rates (dV/dt) of individual grains measured from moving finite element simulations of grain growth with different mobility values, against the rate predicted by the MacPherson–Srolovitz theory. (c) Mean width/(average mean width) distribution. (d) Volume/(average volume) distribution. (e) Area/(average area) distribution. (f) Shape plot for smoothed zirconia mesh.

5. Conclusions

A moving finite element model has been used to simulate grain growth according to curvature-driven interface motion. Both volumetric tetrahedral meshes and surface triangular meshes were used to discretize microstructure; the surface meshes discretize only the grain boundaries. The rates of change of volume of individual grains were measured along with mean widths and triple line edge lengths. Comparisons between the measured rates and those predicted by the MacPherson–Srolovitz theory show good agreement. Mean width is proportional to radius computed from the volume, as expected; variations for individual grains are related to variations in grain shape. Smoothing a mesh obtained from a voxelized reconstruction of a serial sectioning of a sample of zirconia shows that the ratio of L to $V^{1/3}$ decreases as the grains become more compact during the smoothing process. We present a new analysis of grain shape based on ratios between the three basic quantities of volume, area and mean width: a measured microstructure exhibits a different variation between these ratios as compared to a simulated microstructure.

It is a pleasure to acknowledge the debt that ADR owes Prof. Gottstein for numerous in-depth discussions about microstructural evolution in particular and materials science in general over the years. Many aspects of this work started during a sabbatical period at Prof. Gottstein's Institute for Metal Physics and Metallurgy in 2003. The support of the National Science Foundation for this work under contract DMR-0503049 is gratefully acknowledged, as is also the Pennsylvania Infrastructure and Technology Alliance under award 5414138001. Use of facilities provided by the MRSEC at CMU under NSF grant number is DMR-0520425 is also gratefully acknowledged. Support from the Computational Materials Science Network (OBES/DOE) is also gratefully acknowledged.

References

[1] W.E. Reitz: JOM. 50 (1998) 39.
[2] J. von Neumann, in: C. Herring (Ed.), Metal Interfaces, ASTM Cleveland (1952) 108.
[3] W.W. Mullins: J. Appl. Phys. 27 (1956) 900.
[4] J.A. Glazier: Phys. Rev. Lett. 70 (1993) 2170.
[5] W.W. Mullins: Acta Metall. 37 (1989) 2979.
[6] S. Hilgenfeldt, A.M. Kraynik, S.A. Koehler, H.A. Stone: Phys. Rev. Lett. 86 (2001) 2685.
[7] M.E. Glicksman: Philos. Mag. 85 (2005) 3.
[8] P.R. Rios, M.E. Glicksman: Acta mater. 56 (2008).
[9] R.D. MacPherson, D.J. Srolovitz: Nature 446 (2007) 1053.
[10] H. Wang, G. Liu: App. Phys. Lett. 93 (2008) 131902.
[11] L.A. Barrales Mora, G. Gottstein, L.S. Shvindlerman: Acta Mater. 56 (2008) 5915.
[12] J.W. Cahn: Trans. Met. Soc. AIME. 239 (1967) 610.
[13] D. Stoyan, W.S. Kendall, J. Mecke: Stochastic Geometry and Its Applications, John Wiley & Sons, New York (1995)
[14] J.E. Hilliard, in: H. Elias (Ed.), Stereology, Springer-Verlag, Chicago (1967).
[15] D.A. Klain, G.C. Rota: Introduction to Geometric Probability, Cambridge University Press, Cambridge (1997).
[16] J. Gruber, D.C. George, A.P. Kuprat, G.S. Rohrer, A.D. Rollett: Scripta mater. 53 (2005) 351.
[17] J. Gruber: Ph.D. Thesis, Carnegie Mellon University, Pittsburgh (2007).
[18] http://lagrit.lanl.gov
[19] A.D. Rollett, S. Lee, R. Campman, G.S. Rohrer: Ann. Rev. Mater. Res. 37 (2007) 627
[20] Z. Wu, J.M. Sullivan, Jr.: IJNME 58 (2003) 189
[21] K. Andrew: SIAM J. Sci. Comput. 22 (2000) 535.
[22] M.A.H. Cifre: Amer. Math. Monthly. 107 (2000) 893.

(Received August 26, 2008; accepted February 10, 2009)

Bibliography

DOI 10.3139/146.110075
Int. J. Mat. Res. (formerly Z. Metallkd.)
100 (2009) 4; page ■ – ■

ISSN 1862-5282

Correspondence address

Fatma Uyar
Carnegie Mellon University, 5000 Forbes Ave
Materials Science & Engineering Department
Pittsburgh, PA 15213, USA
Tel.: +1 412 736 97 14
Fax: +1 412 268 75 96
E-mail: fuyar@andrew.cmu.edu